I

Publication I

K. Mansikkamäki, P. Ahonen, G. Fabricius, L. Murtomäki, K. Kontturi, Inhibitive Effect of Benzotriazole on Copper Surfaces Studied by SECM, *J. Electrochem. Soc.* **152** (2005) B12-B16.

Journal of The Electrochemical Society, **152** (1) B12-B16 (2005)
0013-4651/2004/152(1)/B12/5/$7.00 © The Electrochemical Society, Inc.

Inhibitive Effect of Benzotriazole on Copper Surfaces Studied by SECM

K. Mansikkamäki, P. Ahonen, G. Fabricius, L. Murtomäki, and K. Kontturi*,z

Laboratory of Physical Chemistry and Electrochemistry, Helsinki University of Technology, FI-02015 HUT, Finland

The inhibitive effect of benzotriazole on a commercial copper surface (phosphorus-deoxidized copper) was studied by a scanning electrochemical microscope (SECM) in an aqueous sodium sulfate solution using ferrocenemethanol (FcMeOH) as the redox mediator. The formation of the inhibitive film was followed as a function of time and as a function of the potential of the copper substrate. The results were analyzed using the existing models in the literature. The results show that the potential has a crucial effect on the growth of the [Cu(I)-BTA] film. At a potential close to the dissolution range of copper, the surface changes gradually from almost ideally conductive to almost ideally insulating surface in the presence of benzotriazole, but at more negative potentials the effect is diminished and finally deceased. Quartz crystal microbalance experiments showed that the mass of an adsorbed layer must correspond to a multilayer.
 [DOI: 10.1149/1.1829413]

Manuscript submitted May 10, 2004; revised manuscript received June 30, 2004. Available electronically November 29, 2004.

The copper industry has used benzotriazole (BTAH) as a corrosion inhibitor for more than 50 years.[1] Today it is widely accepted that it forms a complex layer with Cu(I) ions on the copper surface using Cu-N bonds[2,3] and that it is an anodic-type inhibitor, although it has some inhibitive effect on cathodic oxygen reduction as well.[4] Time, temperature, and the concentration of BTAH has an influence on its inhibitive effect.[4]

In spite of the large consensus of the inhibitive complex film, which BTAH forms with copper, there is, however, still some controversy over the inhibition mechanism of BTAH. The orientation of BTAH on the copper surface and bonding to copper has been widely studied.[3,5-11] The suggested binding mechanism of BTAH with copper can roughly be divided into two alternatives: the orientation of BTAH is either parallel to the surface via the lone pairs of nitrogen and π orbitals[6,7] or perpendicular to the surface using only the lone pairs.[8-10] Some researchers, however, have an intermediate view of the mechanisms. For example, according to Walsh *et al.*,[11] the orientation is tilted rather than perpendicular or parallel to the surface.

Also, the role of oxygen in the adsorption process has been discussed repeatedly. It has been suggested that oxygen is not needed in the initial stages of adsorption of BTAH, but [Cu(I)-BTA] film can be formed onto a clean copper surface.[6,10,12-14] Yet, it has also been claimed that some oxygen is required for adsorption of BTAH.[3,15] It is also stressed that only Cu(I) species are crucial for the formation of an inhibition layer and that no BTAH is adsorbed on the Cu^0 layer.[12]

Several studies of the role of oxygen have been carried out in chloride-containing solutions, and in several cases the copper chloride compound may act as a Cu(I) source. The studies where oxygen is removed simply by bubbling with nitrogen should be taken into account with caution. Copper oxide films start to grow in milliseconds if any oxygen is present in the atmosphere or in the solution, and bubbling the solution with nitrogen is not enough to prepare oxygen-free solutions.

Tromans[2] has calculated the thermodynamic data of [Cu(I)-BTA] films. According to Tromans the rate is affected also by the activities of the reacting species, BTAH and soluble Cu(I) ions which have been formed by anodic processes on the copper surface, and the exposure time of copper to BTAH. Hence, measurements of the growth rate of multilayers are preferably carried out *in situ*.

[Cu(I)-BTA] films have been studied with several electrochemical methods such as impedance spectroscopy[1,16,17] and an electrochemical quartz crystal microbalance (EQCM),[17] as well as various other techniques including X-ray photoemission spectroscopy (XPS),[1,9,10,16] time-of-flight secondary ion mass spectroscopy (TOF-SIMS),[14] scanning electron microscopy (SEM),[16] and surface-enhanced Raman spectroscopy (SERS).[18,19] Microelectrode techniques such as scanning tunnelling microscopy (STM) and scanning electrochemical microscopy (SECM) have been used increasingly in corrosion research,[20] and Cho *et al.*,[6] for example, have studied the orientation of BTAH with STM.

SECM is an effective tool for the study of local electrochemical processes on metal surfaces, such as oxides on Al,[21,22] Ti,[23] or Ta[24] as well as the dissolution kinetics of copper.[25] However, to our knowledge SECM has never been used to study [Cu(I)-BTA] films earlier, even though it allows *in situ* studies of the growing film: the redox activity can be related to the electron tunneling through thin films or the electronic conductivity through thicker films.[21] The basic principles and the modes of operation of the SECM can be found in the literature.[26]

In this communication, SECM has successfully been applied in the study of the formation of [Cu(I)-BTA] film as a function of exposure time and the potential of the copper substrate. The models found in the literature[26-28] have been used to analyze the data. These models relate the oxidation of the mediator at the SECM tip to the reduction of the mediator at the substrate surface. Thus, SECM can also be used to study the changes that occur on the substrate film during exposure time. Also, a few complementary measurements of the rate of adsorption were carried out by EQCM.

Theory

Equations 1 and 2 give the dimensionless current of the tip, when the substrate is ideally insulating or ideally conductive, respectively[26]

$$I_T^{ins} = \frac{1}{0.15 + \frac{1.5358}{L} + 0.58\exp\left(\frac{-1.14}{L}\right) + 0.0908\exp\left(\frac{L - 6.3}{1.017L}\right)} \quad [1]$$

$$I_T^{con} = \frac{0.78377}{L} + 0.3315\exp\left(\frac{-1.0672}{L}\right) + 0.68 \quad [2]$$

where T denotes the tip, and con denotes a conductive and ins an insulating substrate. The dimensionless distance is defined as $L = d/a$ and the dimensionless current is defined as $I = i/i_{lim}$, where i_{lim} is the diffusion-limiting current of the mediator on a disk

* Electrochemical Society Active Member.
z E-mail: kontturi@cc.hut.fi

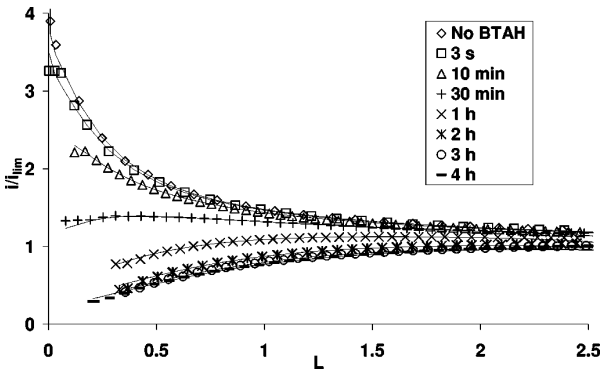

Figure 1. The approach curves measured at the substrate potential of −0.05 V *vs.* SCE. i/i_{lim} is the dimensionless tip current, and $L = d/a$ is the dimensionless distance between the sample and the tip.

ultramicroelectrode placed at an infinite distance from the substrate[26]

$$i_{\text{lim}} = 4nFDca \quad [3]$$

When the reaction at the substrate is under kinetic control, the dimensionless tip and substrate currents can be related by Eq. 4[28]

$$I_{\text{T}} = I_{\text{S}}^{\text{k}}\left(1 - \frac{I_{\text{T}}^{\text{ins}}}{I_{\text{T}}^{\text{con}}}\right) + I_{\text{T}}^{\text{ins}} \quad [4]$$

where

$$I_{\text{S}}^{\text{k}} = \frac{0.78377}{L(1 + 1/\Lambda)} + \frac{0.68 + 0.3315\exp\left(\frac{-1.0672}{L}\right)}{1 + \frac{11/\Lambda + 7.3}{\Lambda(110 - 40L)}} \quad [5]$$

and S denotes the substrate and superscript k for the kinetic control of the reaction. Λ is defined by Eq. 6[27]

$$\Lambda = \frac{k_{\text{S,f}}d}{D_{\text{R}}} = K_{\text{S,f}}L \quad [6]$$

$K_{\text{S,f}}$ denotes the dimensionless heterogeneous rate constant at the substrate surface[28]

$$K_{\text{S,f}} = \frac{ak_{\text{S,f}}}{D_{\text{R}}} \quad [7]$$

A rough estimate of the changes in the thickness of the film can be also calculated as a function of time, if the thickness is assumed to be the only factor that influences the changes of the film resistance. In these cases the apparent $k_{\text{S,f}}$ can be defined as

$$k_{\text{S,f}} = \frac{D_{\text{film}}}{\delta} \quad [8]$$

Experimental

The measurements were carried out with the CHI 900 scanning electrochemical microscope (CH Instruments, TX, USA) using a standard three-electrode cell in normal atmosphere containing oxygen. The reference electrode was a saturated calomel electrode (SCE) and the counter electrode was a Pt wire. The SCE was inserted into the cell with a salt bridge to avoid any chloride ions entering into the measuring solutions. The SECM tip was made of Pt wire (25 μm diam) sealed in a glass capillary (the ratio of the surface area of the sealing glass to the Pt wire, RG, is 6-10, depending on the polishing of the tip). The preparation of the tip is described elsewhere.[29]

The substrate material was commercial phosphorus-deoxidized (DHP) copper received from Outokumpu Copper [composition: Cu min 99.9%, P: 81 ppm (average)]. The copper sample with 5 mm diam was insulated with Teflon and inserted on the bottom of the cell. The substrate was polished both mechanically and electrically. Mechanical polishing was done first with sandpaper (600 grit), then with aluminum micropolish (0.3 μm particle size), and finally using only water and the polishing cloth. Then the sample was rinsed with water and ethanol and electropolished for *ca.* 6 min in a concentrated solution of phosphorus acid and sulfuric acid. The cathode electrode was a copper plate, and the cell potential *ca.* 5 V. After polishing the sample was cleaned in an ultrasonic bath in milli-Q (MQ) water for 10-15 min and twice in ethanol for 20 min.

The measurements were carried out at five different potentials, −0.05, −0.10, −0.15, −0.20, and −0.30 V *vs.* SCE. Both the tip and the copper substrate were polished between each potential. The approach curves were measured as a function of time with and without BTAH (Merck, p.a.), using ferrocenemethanol (FcMeOH, Aldrich) as the mediator and Na_2SO_4 (Merck, p.a.) as the supporting electrolyte. First, 1 mL of a solution of 0.1 M Na_2SO_4 + 1 mM FcMeOH was inserted in the cell, after which the tip was characterized (for RG) with cyclic voltammetry and by measuring an approach curve at an insulating Teflon substrate. Then the tip was moved above the copper surface and the approach curve was measured keeping the copper sample at a predetermined potential. During the approach curve measurements the potential of the tip was held at 0.45 V *vs.* SCE to obtain diffusion-limited tip current.

After measuring the approach curve without BTAH, the solution was removed from the cell and the cell was rinsed twice with MQ water without displacing the tip. Then 1 mL of a solution of 0.333 mM BTAH + 0.0667 M Na_2SO_4 + 0.667 mM FcMeOH was added to the cell and the approach curves were measured 3 s, 10 min, 30 min, 1 h, 2 h, 3 h, and 4 h after the addition. Between the measurements the tip was lifted up for 200 μm from the surface without horizontal displacement. Thus, the measurements were done exactly on the same position of the copper substrate, and the effect of the surface heterogeneity can be neglected when comparing the curves measured at different exposure times. As the tip might have touched the surface in the end of an approach curve, a cyclic voltammogram (CV) was measured after every approach curve to assure that the tip remained intact.

A CV of DHP copper was measured to select the appropriate sample potentials. The measurements were done in the same cell as the approach curves, using the copper sample as a working elec-

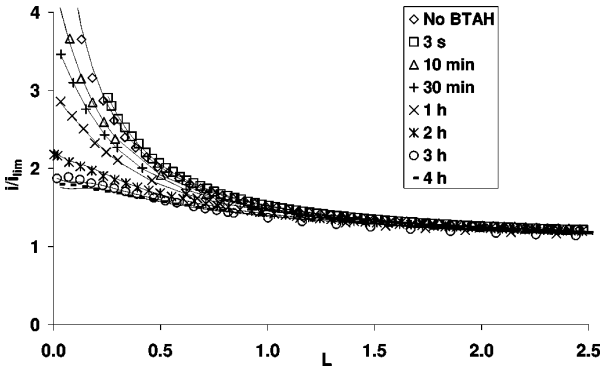

Figure 2. Approach curves measured at the substrate potential of −0.10 V *vs.* SCE. i/i_{lim} is the dimensionless tip current, and $L = d/a$ is the dimensionless distance between the sample and the tip.

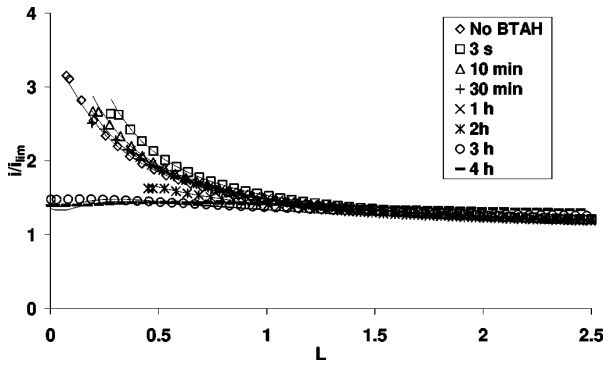

Figure 3. The approach curves measured at the substrate potential of −0.15 V *vs.* SCE. i/i_{lim} is the dimensionless tip current, and $L = d/a$ is the dimensionless distance between the sample and the tip.

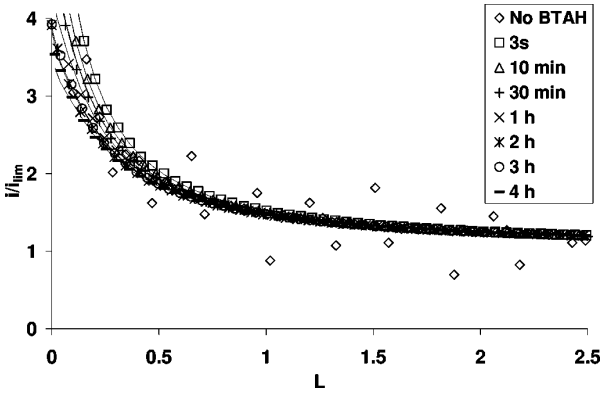

Figure 5. The approach curves measured at the substrate potential of −0.3 V *vs.* SCE. i/i_{lim} is the dimensionless tip current, and $L = d/a$ is the dimensionless distance between the sample and the tip.

trode. The solution was 1 mM FcMeOH + 0.1 M Na_2SO_4 and the sweep rate was 1 mV/s.

The EQCM experiments were carried out with Maxtek PM-700 plating monitor (Maxtek, Inc. CA, USA) with unpolished and electrochemically polished 5 MHz Au crystals. A copper layer was electrolyzed on the Au surface from an aqueous solution containing 0.02 M $Cu(NO_3)$, 0.17 M H_2SO_4, and 0.22 M $HClO_4$ (Merck, analytical grade). A current density of 1.73 mA cm^{-2} was passed through the crystal until the target thickness of 7 μm was achieved, which took *ca.* 4 h. The roughness of the clean Au surface and the electrodeposited copper surfaces after exposing to BTAH was studied with a scanning tunneling microscope (Topometrix, TMX 2000, Explorer Scanning Probe, USA) using tungsten tips. The ratio of the studied clean Au or [Cu(I)-BTA] surface areas and the scanning area were 1.02 and 1.28-1.45, respectively. The deposited Cu layer was first polished mechanically with alumina and thereafter with anodic dissolution in the solution of 66 wt % H_3PO_4 (Merck). The polishing solution containing both sulfuric and phosphoric acid dissolved the thin electrodeposited copper layer too aggressively during the polishing. The cell potential was 2.5 V and the cathode was a copper plate. During the electrolysis and polishing the solutions were vigorously stirred to achieve homogeneous Cu plating which was checked with an ordinary microscope. The adsorption of BTAH was monitored in 0.5 mM or 1.0 mM aqueous BTAH solution.

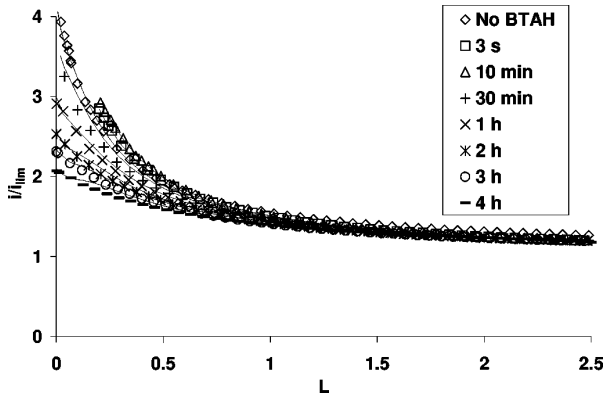

Figure 4. The approach curves measured at the substrate potential of −0.20 V *vs.* SCE. i/i_{lim} is the dimensionless tip current, and $L = d/a$ is the dimensionless distance between the sample and the tip.

Results and Discussion

Figures 1-5 introduce the approach curves. The solid lines in the figures are the results of modeling and the points are measured currents of the tip. Approximately every twentieth point is shown in the figures but the modeling was done using all the points between the range $0.1 < L < 1.5$ in which the model is valid. The potentials have been selected from the passive area of copper in a near-neutral solution. The most positive potential, −0.05 V, is close to the starting point of active dissolution, but the other potentials are clearly in the passive range as the CV measured in the solution of 1 mM FcMeOH + 0.1 M Na_2SO_4 shows (Fig. 6).

The inhibitive effect of BTAH is clearly seen in the figures, because the copper surface changes gradually from an almost ideally conductive to an almost ideally insulating surface when the potential is close to the dissolution range of copper (at −0.050 V). When comparing the curves at different potentials, it is obvious that the potential of the copper substrate affects the formation of the inhibitive complex film. At the most positive potentials the inhibitive film grows fast on the copper surface, but when changing the potential in the cathodic direction, the film growth is decelerated and finally deceased.

When measuring the first approach curve (in the absence of BTAH) at −0.30 V *vs.* SCE, a noisy signal was detected. The noise is probably due to hydrogen evolution and at that potential the oxide may not be so stable as it is at more positive potentials. As already mentioned, oxygen may have a significant role in the adsorption process. If the noise at −0.30 V really is due to breakdown of the

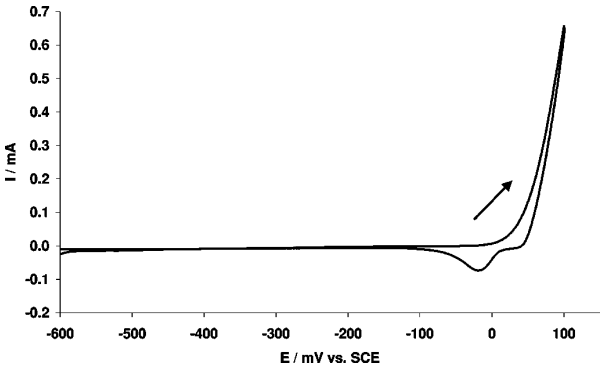

Figure 6. The CV of DHP copper measured in 1 mM FcMeOH + 0.1 M Na_2SO_4 solution. The sweep rate is 1 mV/s.

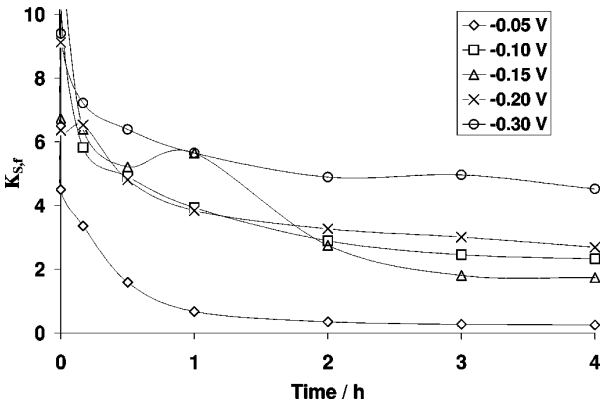

Figure 7. Dimensionless rate constant of the mediator at the substrate surface, $K_{S,f}$, as a function of the exposure time.

oxide film and if the oxygen content on the copper surface decreases, it can be concluded that oxygen seems to be a vital element for [Cu(I)-BTA] film to form. However, the role of oxygen has to be studied in more detail in totally oxygen-free environments, and future studies are planned to be carried out in a nitrogen box. When measuring the approach curves in the presence of BTAH no noise was observed, and even though the growth of [Cu(I)-BTA] film was not observed, BTAH inhibited hydrogen evolution.

The insulating effect of the [Cu(I)-BTA] film may be due to three factors: (*i*) BTAH binds copper atoms that could reduce FcMeOH, (*ii*) ions cannot diffuse from the metal/complex interface to the complex/electrolyte interface (or in the opposite direction), and (*iii*) the conductivity of the film decreases.

The rate constants for the reduction of FcMeOH at the copper surface, $K_{S,f}$ and $k_{S,f}$, were optimized via Eq. 1-6 using a worksheet solver. The optimization is very sensitive to the tip-substrate distance *d*: although in some experiments the tip touched the sample and a shoulder in an approach curve was seen, *d* had to be taken as an adjustable variable in the model. The distance where the shoulder appeared could not be set as the zero distance, because the tip was probably tilted and thus the glass sealing of the tip touched the surface, while the actual Pt electrode was still a couple of micrometers away from the substrate.

The difference between the theoretical distance calculated from the models and the zero distance estimated from the point where the tip may have touched the surface can be estimated. In the beginning of the measurements the difference was maximum 1-2 μm at every potential and in some cases almost 0 μm. However, during the approach curve measurements the tilt may have increased or decreased because of the contact between the tip and the surface. The maximum difference between these two distances was 5 μm (−0.15 V, approach curves measured 2 and 3 h after the addition of BTAH), but in most of the measurements the difference was only 1 μm. Because of these differences the distance was selected to be a modeling parameter.

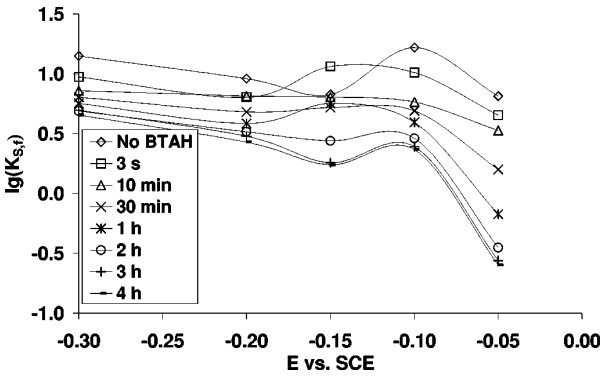

Figure 8. Logarithm of the dimensionless rate constant of the mediator at the substrate surface $K_{S,f}$, as a function of the substrate potential. $K_{S,f}$ can be calculated from the modeling result of the approach curves that are measured both as a function of exposure time to BTAH as well as as a function of potential of the substrate.

Table I. Rate constants and the thickness of the films calculated using the electronic diffusion coefficient after 4 h exposure to the BTAH solution.

E (V *vs.* SCE)	$K_{s,f}$	$10^3 \times k_{S,f}$ (cm s^{-1})	δ (nm)
−0.05	0.25	1.35	29.62
−0.10	2.33	12.47	3.21
−0.15	1.73	9.30	4.30
−0.20	2.69	14.41	2.78
−0.30	4.52	24.24	1.65

Table I shows the dimensionless rate constants, $K_{S,f}$, and the rate constants, $k_{S,f}$, calculated according to Eq. 6, after 4 h exposure to BTAH (*a* is radius of the tip, 12.5 μm, and D_R is diffusion coefficient for FcMeOH, 6.7×10^{-6} cm^2 s^{-1} [2 30]). In the calculations, it is assumed that both the oxidized and reduced species of FcMeOH have the same diffusion coefficient in an aqueous solution. However, the data in Table I is only approximate due to inaccuracy in the distance *d*.

Figure 7 introduces the dimensionless rate constant $K_{S,f}$ as a function of the exposure time. In the beginning of the measurement $K_{S,f}$ decreases rapidly at each potential, and after 1 h no remarkable changes in rate constant are seen. At −0.05 V, where the effect of BTAH is the strongest, $K_{S,f}$ decreases almost exponentially. The thickness of the film can be calculated from $K_{S,f}$ through Eq. 7 and 8, provided that the exact diffusion coefficient of FcMeOH in the film can be estimated. Metikoš-Huković *et al.*[31] have estimated the ionic diffusion coefficient in [Cu(I)-BTA] film to be 4×10^{-14} cm^2 s^{-1}. When this value is used as the apparent diffusion coefficient D_{film}, the thickness of the films after 4 h exposure is about 10^{-5} nm, which is absurd, and it can be concluded that only electrons diffuse through the [Cu(I)-BTA] layer. It is known from the literature that the thickness of the [Cu(I)-BTA] film is approximately 1-200 nm at the open circuit potential.[17,31,32] Beverskog *et al.*[33] have suggested that the ratio of the electronic and the ionic diffusion coefficients in oxide films at room temperature is approximately 10^5. Thus, the apparent electronic diffusion coefficient is approximately 4×10^{-9} cm^2 s^{-1}, and the thicknesses of the [Cu(I)-BTA] films after 4 h exposure are 1.6-29.6 nm (Table I). These values are in good agreement with earlier reported thickness values. For example, according to the impedance measurements of Frignani *et al.*,[17] the thickness is 0.9-180 nm at pH 2.3 in 0.1 M Na_2SO_4 solution, depending on the concentration of BTAH solution.

In Fig. 8 the logarithm of the dimensionless rate constant, $K_{S,f}$, is presented as the function of potential. The nature of the surface has a great effect on these curves: at each potential the measurements are done at the same horizontal position, but the different potentials refer to different positions on the surface and to different surface roughness. This may have an effect on the adsorption process. Even so, the decrease in inhibitive action of BTAH when the potential was changed in the cathodic direction is clearly visible. The logarithm of the dimensionless rate constant decreases as a function of potential at every exposure time and the logarithm is lowest at −0.05 V.

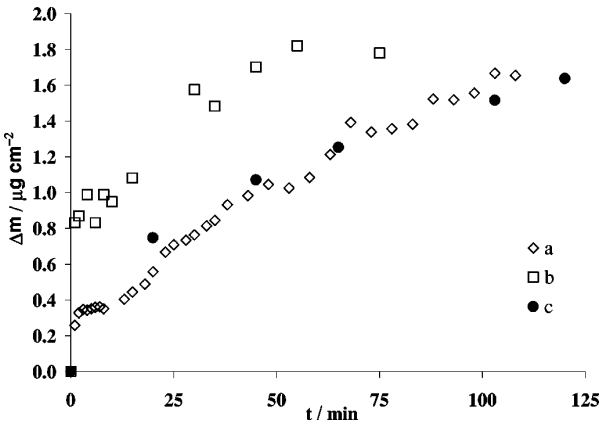

Figure 9. Mass increase due to BTAH adsorption on the copper surface: (a and c) copper is deposited from the solution on the initially unpolished Au crystal, (b) copper is deposited from the solution on the initially polished Au crystal.

Figure 9 shows the increase of mass due to BTAH adsorption measured with EQCM. As can be seen, the mass increase saturates at the level of *ca.* 1.7 $\mu g\,cm^{-2}$ in less than 2 h, and the level is independent of the polishing. However, the level is reached faster with the polished surface than with the unpolished. Using the molecular weight of BTAH the number of molecules adsorbed on the copper surface during the measurement can be calculated. This number corresponds to a mean molecular area of *ca.* 0.017 nm^2, assuming the surface to be the roughest observed with STM. However, using the bond angles and the lengths of the models of Jiang and Adams,[8] the mean molecular area of BTAH can be estimated to be 0.028 nm^2 if the orientation of the molecule is flat or 0.033 nm^2 if the orientation is upright. This indicates that there is more than one monolayer of BTAH on the copper surface, thus providing some support for the calculated values of the apparent film thickness in Table I.

Conclusions

The effect of potential on the adsorption process of BTAH is clearly seen in neutral solution; at the potential close to the dissolution range the almost ideally conductive copper is converted to an almost ideally insulating surface in the presence of BTAH, whereas a shift of potential in the cathodic direction prevents the growth of the [Cu(I)-BTA] film on copper. The insulating film of BTAH grows fast on copper and no significant changes take place in the insulating film after 1-2 h exposure to BTAH solution. Because only the electronic diffusion coefficient gives reasonable results of the thickness of the film, it can be concluded that the [Cu(I)-BTA] film acts both as a physical barrier to ions as well as hindering copper dissolution by binding copper atoms, *i.e.*, BTAH inhibits anodic dissolution sites.

The possibility to study both the growth of [Cu(I)-BTA film] and the nature of the film *in situ* at different sample potentials at the same time makes SECM an effective tool for corrosion research. In addition to the nature of the film, the thickness of the film can also be estimated if the electronic diffusion coefficient is known.

Acknowledgments

The authors greatly acknowledge TEKES (The National Technology Agency of Finland) for financial support. Outokumpu Copper and Outokumpu Research are acknowledged for providing the copper material used in the study.

Helsinki University of Technology assisted in meeting the publication costs of this article.

List of Symbols

a	radius of the tip
c	concentration
d	distance between the tip and the substrate
D_{film}	diffusion coefficient of electronic current carriers inside the film
D_R	diffusion coefficient of the reduced mediator
F	Faraday's constant
I	dimensionless current
$k_{S,f}$	rate constant on the substrate surface
$K_{S,f}$	dimensionless rate constant on the substrate surface
L	dimensionless distance
n	number of electrons

Greek

δ	thickness of the layer
Λ	modeling parameter

References

1. W. Qafsaoui, Ch. Blanc, N. Pébère, A. Srhiri, and G. Mankowski, *J. Appl. Electrochem.*, **30**, 959 (2000).
2. D. Tromans, *J. Electrochem. Soc.*, **145**, L42 (1998).
3. E. M. M. Sutter, F. Ammeloot, M. J. Pouet, C. Fiaud, and R. Couffignal, *Corros. Sci.*, **41**, 105 (1999).
4. P. Yu, D.-M. Liao, Y.-B. Luo, and Z.-G. Chen, *Corrosion (Houston)*, **59**, 314 (2003).
5. Z. D. Schultz, M. E. Biggin, J. O. White, and A. Gewirth, *Anal. Chem.*, **76**, 604 (2004).
6. K. Cho, J. Kishimoto, T. Hashizume, H. W. Pickering, and T. Sakurai, *Appl. Surf. Sci.*, **87/88**, 380 (1995).
7. O. Hollander and R. May, *Corrosion (Houston)*, **41**, 39 (1985).
8. Y. Jiang and J. B. Adams, *Surf. Sci.*, **529**, 428 (2003).
9. J.-O. Nilsson, C. Törnkvist, and B. Liedberg, *Appl. Surf. Sci.*, **37**, 306 (1989).
10. B.-S. Fang, C. G. Olson, and D. W. Lynch, *Surf. Sci.*, **176**, 476 (1986).
11. J. F. Walsh, H. S. Dhariwal, A. Gutiérrez-Sosa, P. Finetti, C. A. Muryn, N. B. Brookes, R. J. Oldman, and G. Thornton, *Surf. Sci.*, **415**, 423 (1998).
12. D. Tromans and R. Sun, *J. Electrochem. Soc.*, **138**, 3235 (1991).
13. J. B. Matos, D. D'Elia, O. E. Barcia, O. R. Mattos, N. Pébère, and B. Trobollet, *Electrochim. Acta*, **46**, 1377 (2001).
14. V. Brusic, M. A. Frisch, B. N. Eldridge, F. P. Novak, F. B. Kaufman, B. M. Rush, and G. S. Frankel, *J. Electrochem. Soc.*, **138**, 2253 (1991).
15. Y. Ling, Y. Guan, and K. N. Han., *Corrosion (Houston)*, **51**, 367 (1995).
16. Y. Feng, K.-S. Siow, W.-K. Teo, K.-L. Tan, and A.-K. Hsieh, *Corrosion (Houston)*, **53**, 389 (1997).
17. A. Frignani, M. Fonsati, C. Monticelli, and G. Brunoro, *Corros. Sci.*, **41**, 1217 (1999).
18. R. Youda, H. Nishihara, and K. Aramaki, *Electrochim. Acta*, **35**, 1011 (1990).
19. H. Y. H. Chang and M. J. Weaver, *Langmuir*, **15**, 3348 (1999).
20. T. Suter and H. Böhni, *Electrochim. Acta*, **47**, 191 (2001).
21. I. Serebrennikova and H. S. White, *Electrochem. Solid-State Lett.*, **4**, B4 (2001).
22. I. Serebrennikova, S. Lee, and H. S. White, *Faraday Discuss.*, **121**, 199 (2002).
23. S. B. Basame and H. S. White, *J. Phys. Chem. B*, **102**, 9812 (1998).
24. S. B. Basame and H. S. White, *Anal. Chem.*, **71**, 3166 (1999).
25. J. V. Macpherson, C. J. Slevin, and P. R. Unwin, *J. Chem. Soc., Faraday Trans.*, **92**, 3799 (1996).
26. A. J. Bard, F.-R. F. Fan, and M. V. Mirkin, in *Electroanalytical Chemistry*, Vol. 18, A. J. Bard, Editor, p. 243, Marcel Dekker, Inc., New York (1994).
27. K. Bogwarth and J. Heinze, in *Scanning Electrochemical Microscopy*, A. J. Bard and M. V. Mirkin, Editors, p. 201, Marcel Dekker, Inc., New York (2001).
28. M. V. Mirkin, in *Scanning Electrochemical Microscopy*, A. J. Bard and M. V. Mirkin, Editors, p. 145, Marcel Dekker, Inc., New York (2001).
29. F.-R. F. Fan and C. Demaille, in *Scanning Electrochemical Microscopy*, A. J. Bard and M. V. Mirkin, Editors, p. 76, Marcel Dekker, Inc., New York (2001).
30. N. Anicet, C. Bourdillon, J. Moiroux, and J.-M. Savéant, *J. Phys. Chem. B*, **102**, 9844 (1998).
31. M. Metikoš-Huković, R. Babić, and I. Paić, *J. Appl. Electrochem.*, **30**, 617 (2000).
32. R. Babić, M. Metikoš-Huković, and M. Lončar, *Electrochim. Acta*, **44**, 2413 (1999).
33. B. Beverskog, M. Bojinov, P. Kinnunen, T. Laitinen, K. Mäkelä, and T. Saario, *Corros. Sci.*, **44**, 1923 (2002).